AN ON-CHIP OPTO-MECHANICAL ACCELEROMETER

B. Dong [1, 2], H. Cai[2], J. M. Tsai[2], D. L. Kwong[2] and A. Q. Liu[1, 2†]
[1]School of Electrical & Electronic Engineering, Nanyang Technological University, Singapore 639798
[2] Institute of Microelectronics, A*STAR (Agency for Science, Technology and Research), Singapore 117685

ABSTRACT

Optically enabled accelerometers offer superior displacement resolution and resilience to electromagnetic interference, which brought benefits to a wide range of applications ranging from inertial navigation to consumer electronics [1, 2]. However, impossible chip scale integration hampered their practical applications [2]. In this paper, a novel in-plane opto-mechanical accelerometer is demonstrated, which employs Whisper Gallery Mode (WGM) ring resonator (RR) as a displacement sensor that monolithically integrated with a nano-tethered proof mass with high mechanical Q-factor. Utilizing design optimized for strong opto-mechanical interactions allows the detection with high sensitivity of 3.279 pm/g at low-power operation.

INTRODUCTION

Accelerometer is always an important device in various applications from consumer electronics to inertial navigation. As the development of silicon microfabrication, silicon based accelerometers are possible due to subsequent cost reduction. [1] Traditionally, microelectromechanical systems (MEMS) accelerometers play a dominant role in accelerometer market due to its low cost and small size, which employs various techniques like piezo-resistive, capacitive and tunneling [1, 3] However, as request for smaller accelerometer and high resolution, research in optical accelerometer is attracting more attention.[4-6] Optically enabled accelerometers offer superior displacement resolution and resilience to electromagnetic interference[1,2]. However, impossible chip scale integration hampered their practical applications [2]. The development of nano-photonics makes the chip scale all optical accelerometer possible.

Currently, most of the optical accelerometer employs free space light modulation [3-6], like grating and diffraction, which require out of plane detection that make it difficult for on-chip integration. As the development of nano-photonics technology [7-8], waveguide type devices are attracting more attention for various applications, which have merits like low loss, small foot print and easily integrated with other devices. Therefore, to overcome the disadvantages of current optical accelerometer, waveguide type displacement sensor is implemented for on-chip signal detection and sensing.

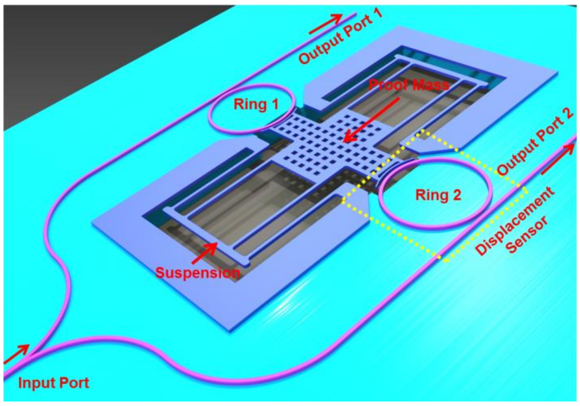

(a)

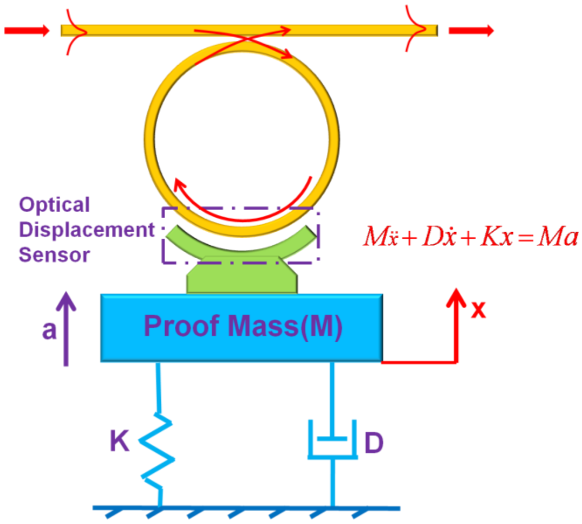

(b)

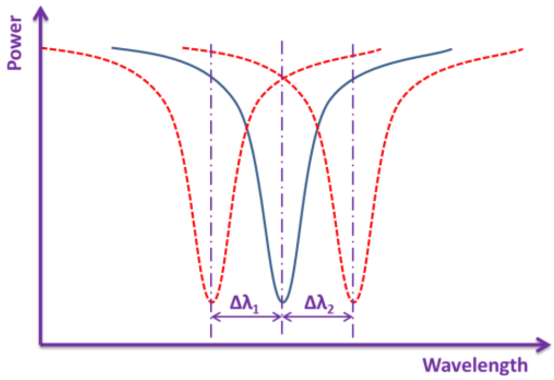

(c)

Fig. 1: (a) Schematic of x-axis opto-mechanical accelerometer. (b) Working principle of the accelerometer with optical distance sensor. (c) Transmission signal under acceleration.

978-1-4673-5655-8/13/$31.00 ©2013 IEEE

MEMS 2013, Taipei, Taiwan, January 20 – 24, 2013

DESIGN AND THEORY

The schematic of the accelerometer is shown in Fig. 1(a), which consists of a proof mass (PM), suspension and two optical displacement sensors. The PM has a dimension of 20 µm × 40 µm, with holes for release purpose. The suspension consists of eight 25 µm × 300 nm silicon beams. There are two symmetrically distributed displacement sensors, with each constructed by a ring resonator (RR) and an arc. The RR has a diameter of 60 µm, with a high Q-factor up to 13,000. The accelerometer is fabricated on SOI wafer with 220 nm silicon structure layer. Broad band light is coupled into the input port, and split into two waveguides, which the ring resonators are coupled with. After the displacement sensor, the modulated light is detected and compared at the output port.

The working principle is the optical accelerometer is shown in Fig. 2(b). Generally, the accelerometer is governed by the equation:

$$M\frac{d^2x}{dt^2}+D\frac{dx}{dt}+Kx=F=Ma \tag{1}$$

where M is the weight of the proof mass, D is the damping factor and K is the spring constant.

For accelerometer, two important parameters are sensitivity and bandwidth. At frequency well below the resonance, the displacement of the PM is proportional to the acceleration; therefor the static sensitivity of the accelerometer can be expressed as [3]:

$$\frac{x_{static}}{a}=\frac{M}{K}=\frac{1}{\omega_r^2} \tag{2}$$

where is ω_r is the nature resonance frequency shown as:

$$\omega_r=\sqrt{\frac{K}{M}} \tag{3}$$

By observing the above two equations, it is evident that there is trade-off between bandwidth and sensitivity [1-3]. Natural frequency must be low for high sensitivity and to achieve a high sensitivity, the mass must be increased while reducing the stiffness of the spring.

The optical displacement sensor consists of a nano-waveguide, a ring resonator and an arc. The arc is connected with the proof mass and move together upon acceleration. The gap (g) between the arc and ring changes as

$$g=g_0\pm\Delta x \tag{4}$$

where g_0 is the initial gap between the ring and arc, which is 150nm. The resonance wavelength of the ring resonator is linearly related with the effective refractive index (n_{eff}). Changing in the effective refractive index induce shift of resonance wavelength. The effective refractive index and gap is related through the optomechanical coupling coefficient (g_{om}) which is defined as [7]

$$g_{om}=\frac{\Delta\omega}{\Delta x} \tag{5}$$

The resonance frequency (ω) of the RR shifts because of the change in position of the arc due to evanescent wave perturbation. Upon acceleration, the PM undergoes a displacement, leading to a change of the gap (*gap*) between the RR and arc. As a result, the transmission signal at ring 1 and 2 will shift in the opposite direction because the gap changes in the opposite direction as shown in Fig. 1(c). The measured wavelength difference ($\Delta\lambda_1$ + $\Delta\lambda_2$) is induced by the acceleration, which doubled the sensitivity as compared to a single ring.

Fig. 2 illustrates the principle of the optical displacement sensor. The resonant wavelength of the RR is determined by its effective refractive index (n_{eff}); the n_{eff} decreases when the *gap* increases. The insert shows the electrical field distribution for TE mode, which is enhanced in the gap, and its distribution is quite sensitive to the gap. Fig 2(b) shows that the change of n_{eff} is also related with gap. In order to have a high change in effective refractive index, small gap is necessary, which require better lithography and fabrication technology.

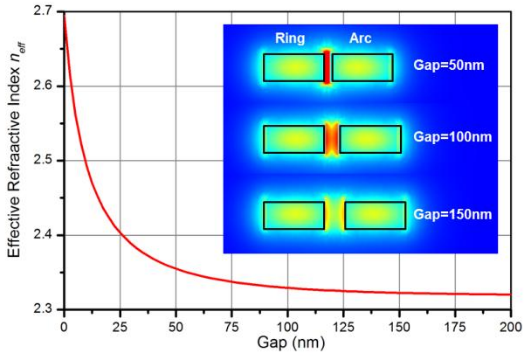

(a)

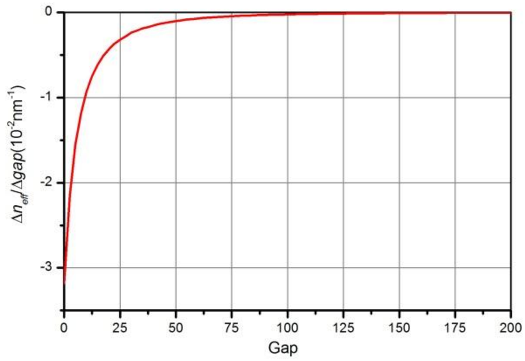

(b)

Fig. 2: (a) Effective refractive index changes as a function of gap. (b) Change of effective refractive index as a function of gap.

Therefore, upon acceleration, the resonant wavelength shifts as a consequence of PM's displacement, which is shown in Fig. 3. The mechanical displacement shows a very good linearity because the displacement is relatively small (less than 1 nm) as compared to the gap (150 nm). Due to small displacement, the effective refractive index changes lineally at g_0 equal to 150 nm, resulting a linear wavelength shift. The wavelength shifts 3.279 nm/g for a single RR while the PM moves at 22 pm/g. Due to double RRs, a signal difference at output port can give double sensitivity, which can improve the performance of the accelerometer.

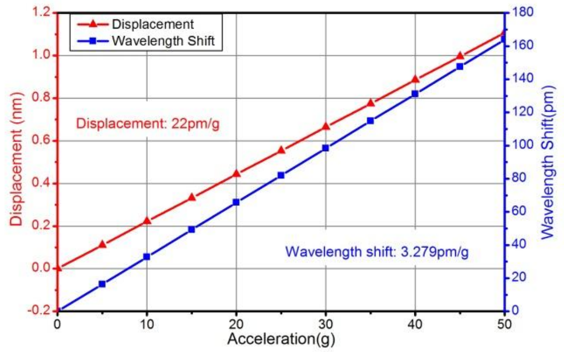

Fig.3: PM displacement and wavelength shift under acceleration.

Another important parameter of accelerometer is frequency response, which determines the working bandwidth of the device. Fig. 4 shows the frequency response of the accelerometer at various damping condition. Due to the small dimension of the accelerometer, it has a high eigenfrequency (f_m = 103 kHz), which corresponds to a high operating bandwidth, up to 30 kHz at critical damping. The damping rate can be controlled by optical gradient force [2, 7-8] between the ring and arc, which provides an easy way to calibrate the accelerometer.

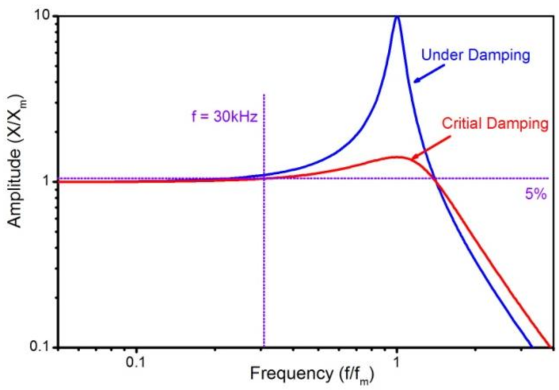

Fig. 4: Frequency response of the accelerometer.

FABRICATION

Fig. 5 shows the scan electron microscope (SEM) images of the accelerometer and optical displacement sensor. The accelerometer is fabricated via C-MOS compatible nano-photonics fabrication technology. Starting with standard SOI wafer with 220nm silicon layer and 2 µm buried oxide layer, followed by deep-UV lithography and plasma etch. All structures, such as proof mass, springs and ring resonators, are patterned via lithography with minimum feature size around 150 nm. After silicon etch, a 2 µm oxide layer are deposited symmetrically on top to silicon patterns via PECVD to reduce the propagation loss, followed by 100 nm amorphous silicon layer, which define the released window pattern. HF vapor are employed to undercut the cladding and buried oxide in the released window.

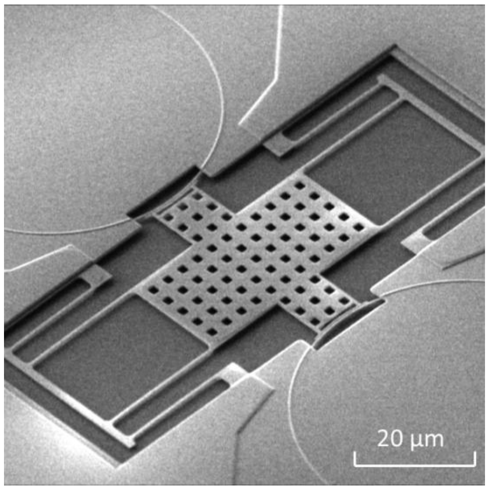

(a)

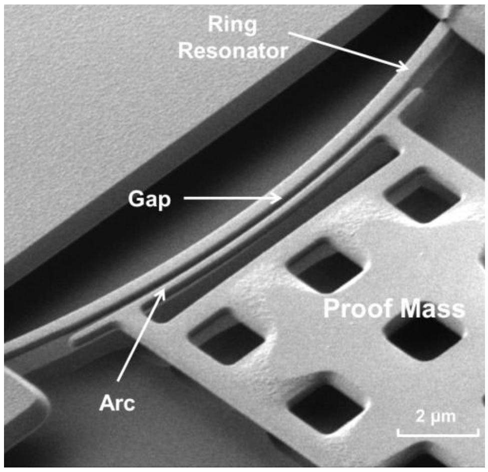

(b)

Fig. 5: SEM images of the (a) optical accelerometer and (b) optical displacement sensor.

EXPERIMENTS AND DISCUSSIONS

Fig. 6 shows the transmission spectrum of the accelerometer at ± g. The sample is tested with different orientations, and the transmission spectra for one ring are recorded. The tested sensitivity is approximately 15 pm/g, which is higher as compared to the simulated sensitivity (3.279 pm/g).

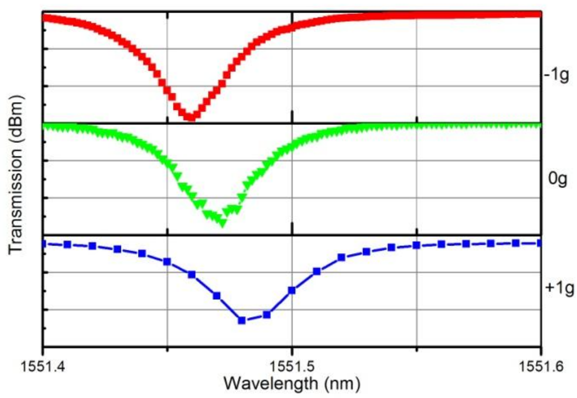

Fig. 6: Transmission spectrum of the accelerometer at ±g.

To further increase the sensitivity, the proof mass can be increased while reducing the stiffness of the silicon beams by better spring design. Beside this, the optical displacement sensor can be more sensitive to displacement by e-beam lithography, which can reduce the minimum feature size below 100 nm, which can provide superior resolution.

CONCLUSIONS

In conclusion, an on-chip opto-mechanical accelerometer is designed, fabricated and experimentally demonstrated. Fabricated with CMOS compatible process, this optical accelerometer can be easily packaged and integrated with other photonic devices. Optical displacement sensor with WGM ring resonator promises a high resolution. The opto-mechanical accelerometer can be potentially used at hash environment like in oil industry, or military usage in a complex electromagnetic environment. It has other potential applications such as optical resonator type gyroscope and mechanical force sensor.

ACKNOWLEDGEMENTS

The authors would like to acknowledge the support from by Environmental & Water Industry Development Council of Singapore (MEWR C651/06/171) and the Science and Engineering Research Council of A*STAR (Agency for Science, Technology and Research), SERC Grant 1021650084.

REFERENCES

[1] G. Krishnan, C. U. Kshirsagar, G. K. Ananthasuresh and N. Bhat, "Micromachined high-resolution accelerometers", J. Indian Inst. Sci., vol. 87, pp. 333–361 (2007).

[2] A. G. Krause, M. Winger, T. D. Blasius, Q. Lin, and O. Painter, "A high-resolution microchip optomechanical accelerometer", Nature Photonics, vol. 6, pp. 768-772, 2012.

[3] N. Yazdi, F. Ayazi, and K. Najafi, "Micromachined inertial sensors," Proceedings of the IEEE, vol. 86, pp. 1640-1659, 1998.

[4] E. B. Cooper, E. R. Post, S. Griffith, J. Levitan, S. R. Manalis, M. A. Schmidt, and C. F. Quate, "High-resolution Micromachined Interferometric Accelerometer," Applied Physics Letters, vol. 76, No. 22, pp. 3316–3318, 2000.

[5] N. C. Loh, M. A. Schmidt and S. R. Manalis, "Sub-10 cm^3 Interferometric Accelerometer with Nano-g Resolution", Journal of Microelectromechanical Systems, vol. 11, No. 3, pp. 182-187, 2002.

[6] U. Krishnamoorthy, R. H. Olsson Iii, G. R. Bogart, M. S. Baker, D. W. Carr, T. P. Swiler, and P. J. Clews, "In-plane MEMS-based nano-g accelerometer with sub-wavelength optical resonant sensor," Sensors and Actuators A: Physical, vol. 145–146, pp. 283-290, 2008.

[7] M. Li, W. H. P. Pernice, C. Xiong, T. Baehr-Jones, M. Hochberg, and H. X. Tang, "Harnessing optical forces in integrated photonic circuits," Nature, vol. 456, pp. 480-U28, Nov 2008.

[8] D. Van Thourhout, and J. Roels, "Optomechanical device actuation through the optical gradient force," Nature Photonics, vol. 4, no. 4, pp. 211-217, 2010.

CONTACT

*A. Q. Liu, Tel: +65-67904336; eaqliu@ntu.edu.sg